

# Coherent control of mesoscopic tunneling

Christoph Weiss\* and Tharanga Jinasundera

*Institut für Physik, Carl von Ossietzky Universität, D-26111 Oldenburg, Germany*

(Dated: November 11, 2018)

For a weakly interacting Bose-Einstein condensate in a double well, an appropriate time-dependent modulation of the trapping potential counter-acts the “self-trapping” effects of the interactions, thereby allowing tunneling between the wells. It is demonstrated numerically that this modulation can be employed for transferring the condensate from one well to the other in a controlled way. Moreover it allows the production of mesoscopic entangled states on short time scales.

PACS numbers: 03.75.Lm, 05.30.Jp, 32.80.Pj

## I. INTRODUCTION

Bose-Einstein condensates in double well potentials display a wide variety of important phenomena, ranging from interference of two condensates released from a double well trap [1] and the relative phase of two condensates [2] over the Josephson effect [3, 4, 5, 6] to parametric resonance [7]. In this paper, we demonstrate that the tunneling effect between the two condensates can systematically be manipulated by an appropriate time-dependent variation of the double well potential.

For a single particle in a double well, it has been shown that the tunneling effect can be coherently destroyed by an external oscillating force [8]. A similar effect has also been predicted for condensates [9]. Here, we pursue the opposite direction: We demonstrate numerically that under the influence of a suitably designed force tunneling of condensates can take place even under conditions where it normally is inhibited by self-trapping.

Self-trapping has only recently been observed experimentally for condensates in a double well potential [10]; the ability to control tunneling in such systems will enable the experimental realization of new phenomena. As a particular application of our technique, we produce numerically highly entangled mesoscopic superpositions (an entangled state cannot be written as a product state). While possible applications of mesoscopic entangled states include interferometry, frequency standards and quantum information processing, the realization of mesoscopic superpositions of condensates is still a challenge of fundamental research. So far, superpositions of single atom states [11], four wave mixing of matter waves [12] and even more complicated quantum states showing multi-particle entanglement [13] have been realized experimentally. There have been several suggestions to produce mesoscopic entanglement with condensates by manipulating the interaction between the particles, or by controlling the dynamics of the system [14, 15, 16, 17, 18, 19]. The method presented here is quite simple, and robust against small uncertainties in both the preparation of the initial state and specific de-

tails of the force. It also might lend itself to a systematic adaption of highly successful methods developed in the field of coherent control of molecular dynamics [20, 21] to condensates.

Our material is organized as follows: First we introduce the  $N$ -particle model used to describe the dynamics, and transform the  $N$ -particle Schrödinger equation into an equivalent set of equations. These equations reveal the guiding principle how to design the required time-dependent forces (a discussion of the validity of the model can be found in the appendix). We then demonstrate numerically how an efficient population transfer from one well to the other can be achieved, and outline the strategy of creating mesoscopic entanglement.

## II. MODEL

For a matter-of-principle discussion, we consider the  $N$ -particle Hamiltonian

$$\hat{H} = -\frac{\hbar\Omega}{2} (\hat{b}_1\hat{b}_2^\dagger + \hat{b}_1^\dagger\hat{b}_2) + \hbar\kappa (\hat{b}_1^\dagger\hat{b}_1^\dagger\hat{b}_1\hat{b}_1 + \hat{b}_2^\dagger\hat{b}_2^\dagger\hat{b}_2\hat{b}_2) + \hbar\mu f(t) (\hat{b}_1^\dagger\hat{b}_1 - \hat{b}_2^\dagger\hat{b}_2), \quad (1)$$

where the Bose operators  $\hat{b}_j^{(\dagger)}$  annihilate (create) one particle in the  $j$ -th well ( $j = 1, 2$ ). In addition,  $\Omega$  denotes the single-particle tunneling frequency,  $\hbar\kappa$  is the on-site interaction energy, and  $\hbar\mu f(t)$  specifies an externally applied potential difference between the two wells. Without this time-dependent modulation, this Hamiltonian is well established for describing the tunneling dynamics of a condensate in a double well potential within a two-mode approximation [22, 23]. The time-dependent force has to be chosen such that this approximation is not violated.

Considering two harmonic wells with angular frequency  $\omega$  and oscillator length  $\ell_{\text{osc}} = \sqrt{\hbar/(2m\omega)}$  separated by a distance of  $2d$ , conservative estimates [23, 24] yield  $\Omega \simeq \omega\sqrt{2/\pi}d/\ell_{\text{osc}} \exp(-0.5d^2/\ell_{\text{osc}}^2)$  and  $\kappa \simeq \hbar a/(4\sqrt{\pi}m\ell_{\text{osc}}^3)$ , where  $m$  is the atomic mass and  $a$  the  $s$ -wave scattering length. Taking  $^{23}\text{Na}$  atoms with  $a = 2.75$  nm, we obtain  $N\kappa \simeq 1.6\Omega$  for  $N = 1000$  particles by choosing  $\ell_{\text{osc}} \simeq 31.78\mu\text{m}$  and  $d = 3.2\ell_{\text{osc}}$ , say, with  $\omega \simeq 1.362$  Hz,  $\Omega \simeq 0.02078$  Hz. Experimentally,

\*Electronic address: weiss@theorie.physik.uni-oldenburg.de

time-scales shorter by two orders of magnitude can easily be obtained by either choosing just  $N = 100$  or by reducing the interaction with a Feshbach resonance by a factor of 10. In both cases one would have:  $\omega \simeq 136.2$  Hz and  $\Omega \simeq 2.078$  Hz with  $\ell_{\text{osc}} \simeq 3.178\mu\text{m}$  and  $d = 3.2\ell_{\text{osc}}$ .

Without interaction between the particles ( $\kappa = 0$ ), and without any applied force ( $\mu f(t) = 0$ ), an initial state with all particles trapped in one well simply leads to Rabi-like oscillations of the entire population between both wells:  $\langle \hat{b}_1^\dagger \hat{b}_1 \rangle / N = (1 \pm \cos(\Omega t)) / 2$ . For describing the evolution of the interacting system, we use the Fock basis  $|\nu\rangle \equiv |N - \nu, \nu\rangle$  with  $\nu = 0 \dots N$ , so that the label  $\nu$  refers to a state with  $N - \nu$  particles in well 1, and  $\nu$  particles in well 2. The Hamiltonian (1) then becomes a sum of two  $(N + 1) \times (N + 1)$ -matrices,

$$H = H_0(t) + H_1. \quad (2)$$

The non-diagonal matrix  $H_1$  describes the tunneling,

$$\langle \nu | H_1 | n \rangle = -(\delta_{\nu, n-1} + \delta_{\nu-1, n}) \frac{\hbar\Omega}{2} \sqrt{N-\nu} \sqrt{\nu+1}, \quad (3)$$

whereas the diagonal matrix  $H_0$  includes both the interaction between the particles and the applied force,

$$\begin{aligned} \langle \nu | H_0(t) | n \rangle &= \delta_{\nu, n} [(N - \nu)(N - \nu - 1) + \nu(\nu - 1)] \hbar\kappa \\ &+ \delta_{\nu, n} (N - 2\nu) \hbar\mu f(t). \end{aligned} \quad (4)$$

To solve the Schrödinger equation

$$i\hbar \frac{\partial}{\partial t} |\psi(t)\rangle = (H_0(t) + H_1) |\psi(t)\rangle, \quad (5)$$

we employ the ansatz

$$\langle \nu | \psi(t) \rangle = a_\nu(t) \exp \left[ -\frac{i}{\hbar} \int_0^t \langle \nu | H_0(t') | \nu \rangle dt' \right]. \quad (6)$$

A few lines of simple algebra then lead to

$$\begin{aligned} i\hbar \dot{a}_\nu(t) &= \langle \nu | H_1 | \nu+1 \rangle h_\nu(t) a_{\nu+1}(t) \\ &+ \langle \nu | H_1 | \nu-1 \rangle h_{\nu-1}(t)^* a_{\nu-1}(t), \end{aligned} \quad (7)$$

where we have set  $a_{-1}(t) \equiv a_{N+1}(t) \equiv 0$ , and introduced the phase factors

$$h_\nu(t) = \exp \left\{ i \left[ 2(N - 1 - 2\nu)\kappa t + 2\mu \int_0^t f(t') dt' \right] \right\}. \quad (8)$$

This set of differential equations is mathematically equivalent to the  $N$ -particle Schrödinger equation governed by the Hamiltonian (1). It will enable us to design force functions  $\mu f(t)$  to achieve the desired control of tunneling. These predictions will then be tested numerically.

If initially all particles are stored in one well, and no force is applied ( $\mu f(t) \equiv 0$ ), tunneling is inhibited for  $N\kappa/\Omega > 1$ . This self-trapping effect, which originally has been established on the mean-field level [3, 23, 25, 26], has recently been observed experimentally for

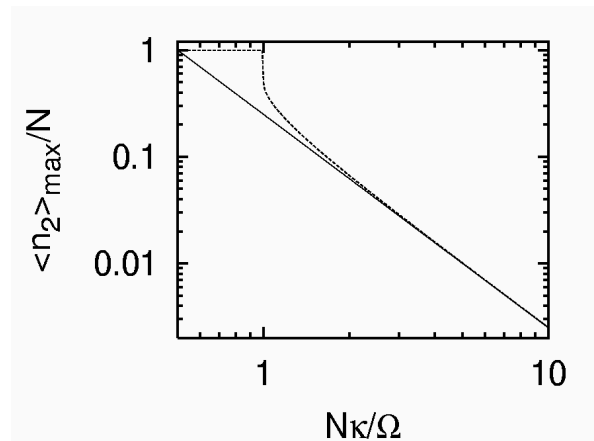


FIG. 1: Maximum fraction of particles found in well 2, after initially all particles had been prepared in well 1, if no force is applied. Solid line: Prediction from Eq. (10) for  $N \gg 1$ . Dashed line: data obtained from the solution of the non-linear Schrödinger equation. There is a self-trapping transition for  $N\kappa = \Omega$  [25, 26].

condensates [10]. Self-trapping can also be understood within the  $N$ -particle approach (*cf.* Ref. [27]): Here, we start with a perfectly trapped situation, in which  $a_\nu(0) = \delta_{\nu,0}$ . In the spirit of time-dependent perturbation theory, we then have to zeroth order  $a_\nu(t) = \delta_{\nu,0}$  for all times. In first order perturbation theory, we obtain  $a_0(t) \simeq 1$ ,  $a_2(t) \simeq 0$ ,  $a_3(t) \simeq 0$ ,  $\dots$ , and

$$a_1(t) \simeq i \frac{\Omega}{2} \sqrt{N} \int_0^t \exp[-i2(N-1)\kappa t'] dt'. \quad (9)$$

Therefore, for not too large  $\Omega/[(N-1)\kappa]$ , the fraction of particles in well 1 evolves in time as

$$\frac{\langle \hat{b}_1^\dagger \hat{b}_1 \rangle}{N} \simeq 1 - \left( \frac{\Omega}{2(N-1)\kappa} \right)^2 \sin^2[(N-1)\kappa t], \quad (10)$$

so that the transfer of population is suppressed. Surprisingly, this perturbative reasoning qualitatively describes self-trapping already for comparatively large  $\Omega/[(N-1)\kappa]$ ; for  $N\kappa > 1.5\Omega$  even the quantitative agreement is good (see Fig. 1).

### III. TRANSFER OF BOSE-EINSTEIN CONDENSATES

We now consider the question how to transfer the condensate from one well to the other even under conditions of self-trapping. If there is no interaction, and all particles are confined in well 1 at  $t = t_0$ , the  $a_\nu(t)$  which are essentially different from zero are centered around  $\nu_c(t) = N(1 - \cos[\Omega(t - t_0)]) / 2$ , as a consequence of the unperturbed Rabi oscillation. To reproduce this behavior in the interacting case, even in the self-trapping regime, the phase factor  $h_{\nu_c}$  has to remain constant at least for

small time differences  $\Delta t$ . From Eq. (8), this requirement leads to the condition

$$1 \simeq \exp \{i(2N\kappa \cos[\Omega(t - t_0)] + 2\mu f(t))\Delta t\} . \quad (11)$$

To transfer a condensate initially prepared in well 1, we therefore design the force

$$\mu f(t) = \begin{cases} -\mu_0 & : t \leq t_0 \\ \mu_1 \cos[\Omega(t - t_0)] & : t_0 < t < t_0 + \pi/\Omega \\ \mu_0 & : t \geq t_0 + \pi/\Omega \end{cases} , \quad (12)$$

with  $\mu_1 \approx -N\kappa$ . Fortunately, the resulting transfer is reasonably insensitive with respect to the precise value of  $\mu_1$ , as the system still performs Rabi-like oscillations for small but finite interactions. As in the experiments reported in Ref. [10], the role of the constant offset  $\mu_0$  is to prevent tunneling before and after the controlled evolution of the condensate. This offset is an auxiliary device since it merely serves to eliminate the tunneling contact; the same effect could be achieved by increasing the barrier. Our numerical simulations show that  $\mu_0$  and  $\mu_1$  can be chosen such that the experimentally uncertain value of the onset of the pulse  $t_0$  is only of minor importance. We determine the optimal values for  $\mu_0$  and  $\mu_1$  numerically; however, slight deviations from the values given below will lead only to minor deteriorations of the quality of transfer.

For the experimentally realistic parameter combination  $N\kappa = 1.6\Omega$  we use the Shampine-Gordon routine [28] to numerically solve the Schrödinger equation. The only difference between the solutions of the  $N$ -particle Schrödinger equation and its mean field analog (the non-linear Schrödinger equation) is a collapse of the well-to-well oscillations on the  $N$ -particle level for large times which will be followed by a revival [23]; the  $N$ -particle dynamics displays, on short times scales, a self-trapping which is at least as good as on the mean field level. We get good results for the transfer if we choose  $\mu_1 = -2.05\Omega$  and  $\mu_0 = \mu_1$ , as shown in Fig. 2. However, neither trapping nor transfer is perfect then. For a very weakly coupled double well system, we can apply much larger constant forces. This will increase the effective interaction, and therefore the trapping both before and after the tunneling process (*cf.* Eq. (10)). Choosing  $\mu_1 = -1.8\Omega$  and  $\mu_0 = 10\mu_1$  leads to a transfer of more than 99% of the particles (see Fig. 2). In essence, the transfer is achieved by choosing the force-function such that the interaction is effectively switched off for the dominant part of the multi-particle wave-function, according to a neutralization of the phase factors (8) for the most important indices  $\nu$ .

#### IV. GENERATION OF MESOSCOPIC ENTANGLEMENT

In what follows we exploit this possibility of effectively switching off the interaction to produce mesoscopic superpositions (for various measures of entanglement see

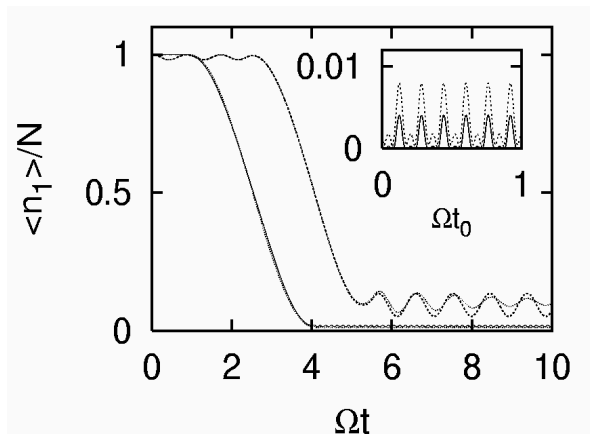


FIG. 2: Population transfer as a function of time obtained for pulses given by Eq. (12). Dashed line: numerical solution of the equation of motion in the mean field approximation for  $\mu_1 = -2.05\Omega$  and  $\mu_0 = \mu_1$ . Solid line: numerical solution of the mean field equation for  $\mu_1 = -1.8\Omega$  and  $\mu_0 = 10\mu_1$ . In both cases, the parameter  $t_0$  was chosen such that we obtain a worst case-scenario as far as trapping of the final state is concerned ( $\Omega t_0 = 0.92$  and  $\Omega t_0 = 2.4$ , respectively). Solutions of the  $N$ -particle Schrödinger equation for  $N = 1000$  (dotted lines) confirm the validity of the mean field approximation. Inset: For the second scenario, the maximum and minimum value of trapping are plotted as a function of the onset of the pulse  $t_0$  (obtained from the mean field equation). The transfer to well 2 varies between better than 99% and 99.9%.

*e.g.* Ref. [29] and references therein). Our strategy consists of two steps: First, an initial state has to split into two parts. Secondly, we separate both parts by an appropriate pulse. The initial splitting is already achieved by starting with a state which is approximately a Fock state  $|n\rangle$  with  $N - n$  particles in well 1 and  $n$  particles in well 2. For  $n = N/2$  and no applied force, the probability distribution  $|a_\nu|^2$  then evolves automatically into a bimodal distribution (*cf.* *e.g.* Ref. [18]), so that the state evolving from a Fock state already displays entanglement. A measure for the “quality” of entanglement is the distance  $\Delta\nu$  between the two maxima. Fortunately, the numerical results of entanglement generation are robust against small uncertainties in the preparation of the initial state.

For a superposition of distinct Fock states, the degree of entanglement does not depend on the phases with which the individual states contribute to the total wave-function. To characterize such an entangled superposition more thoroughly, we perform a gedanken experiment by considering the outcome of all possible measurements of the number  $\ell$  of particles found in well 1. We then take the average of all measurements with  $\ell < N/2$  and call the resulting quantity  $\langle \ell \rangle_<$ . Analogously, let  $\langle \ell \rangle_>$  be the average over all measurements with  $\ell > N/2$ . An ideal entangled state  $(|0\rangle + |N\rangle)/\sqrt{2}$  would thus be characterized by  $\langle \ell \rangle_< = 0$  and  $\langle \ell \rangle_> = N$ . Following the evolution of an initial Fock state numerically, we find that

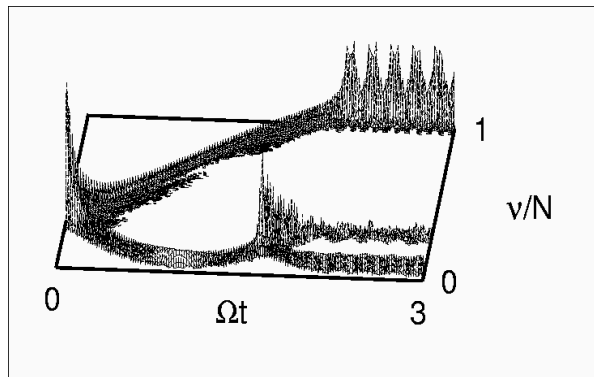


FIG. 3: Mesoscopic superposition evolving from an initial Fock state with 75% of the particles in well 1 and 25% in well 2, under the pulse specified by Eq. (13). Parameters are  $N\kappa = 1.6\Omega$  and  $N = 1000$ . In this plot, probabilities  $|a_\nu(t)|^2$  larger than 0.2% are displayed as a function of both time  $t$  and Fock state index  $\nu$ .

$\langle \ell \rangle_> - \langle \ell \rangle_<$  oscillates in time. For the particular initial state  $|N/2\rangle$  and  $\kappa = 0$ , we obtain  $\langle \ell \rangle_> - \langle \ell \rangle_< < 0.637N$ . Thus, even in the non-interacting case and without any applied force, simply letting an initial Fock state evolve will never lead to a perfect superposition of  $|N\rangle$  and  $|0\rangle$ . Somewhat surprisingly, for an interacting system in the self-trapping regime, better results can be obtained if we start with, say, 75% of the particles in well 1 and 25% in well 2. Initially, roughly half of the dominant squared amplitudes  $|a_\nu|^2$  describing the many-particle wave function will move towards lower  $\nu$ , the other half towards larger  $\nu$ . To separate these two parts, we apply a pulse such that the interaction is effectively switched off for that part which shifts towards higher  $\nu$ ; when the other half of the wave-function is “reflected” at  $\nu = 0$ , the force should be such that trapping sets in soon. This intuitive scenario is implemented through the force function

$$\mu f(t) = \begin{cases} -N\kappa \cos[\Omega(t + t_1)] & : 0 \leq t < \pi/\Omega - t_1 \\ \mu_0 & : t \geq \pi/\Omega - t_1 \end{cases}, \quad (13)$$

with  $\frac{1}{2}(1 - \cos(\Omega t_1)) = \frac{\mu_0}{N}$ . The constant offset  $\mu_0$  is again meant to increase the trapping. However, now we require strong trapping both for  $\nu \approx N$  and  $\nu \approx 0$ . Thus, a parameter  $\mu_0$  of the order of  $N\kappa$  will not do — either an offset with a modulus of, say,  $10N\kappa$  can be applied, or no offset at all. Figure 3 depicts the evolution of the probabilities  $|a_\nu(t)|^2$  for finding  $\nu$  particles in well 2 under the influence of the force (13) with  $N\kappa = 1.6\Omega$  and  $N = 1000$ , and confirms in detail the above qualitative reasoning: The distribution develops pronounced maxima at both low and high  $\nu$ . For the final state, we have  $\langle \ell \rangle_> - \langle \ell \rangle_< > 0.73N$ .

Thus, while the final state still is no perfect entangled state, we have demonstrated that our strategy is capable of producing states which at least come close to the theoretical ideal. From the numerical estimates stated above for  $^{23}\text{Na}$ , we infer that the production time

$3/\Omega \simeq 40$  ms is shorter than typical experimental coherence times [1, 10, 30]. Creating and studying mesoscopic superpositions of condensates might greatly improve our knowledge of the achievable degree of coherence in mesoscopic systems. In a laboratory experiment, the required initial Fock state could be prepared by involving a constant potential offset between the two wells, in order to prevent untimely onset of tunneling [10]. Our numerical data confirm that the resulting state depends only weakly on the particular moment when this offset is switched off.

## V. CONCLUSION

To conclude, we have shown numerically that a suitably designed time-dependent modulation of a double well potential can partially eliminate the effect of the interaction between the particles of a trapped Bose-Einstein condensate. This finding can be exploited for achieving a controlled tunneling transfer of the condensate from one well to the other, or for preparing mesoscopic entangled states. While here we have guessed the shape of the modulation by mere inspection of the phase factors (8), in order to establish the principal feasibility of our strategy, the result might be optimized if an analysis of the final state is employed, by means of a feedback loop, to design more efficient pulses. Thus, we suggest to employ the techniques which have already been developed and successfully applied to the coherent control of molecular dynamics by specifically designed laser pulses [20, 21] to the coherent control of condensates in specifically modulated double-well potentials.

## Acknowledgments

We would like to thank M. Holthaus for initiating this project and S. Trotzky for help with the calculations in the appendix. Support from the DFG Priority Programme SPP 1116, “Interactions in ultracold atomic and molecular gases”, is gratefully acknowledged.

## APPENDIX A: VALIDITY OF THE TWO-MODE APPROXIMATION

In order to demonstrate the validity of the two-mode approximation, we repeat the mean field calculations for a non-linear Schrödinger equation also in a four-mode approximation (to do the  $N$ -particle calculations in a four-mode approximation for 1000 particles exceeds the capacity of most available computers). Throughout the appendix, we assume that the individual wells can be described by harmonic oscillators. The validity of the two-mode approximation is not restricted to this situation. However, to go beyond the two-mode approximation, assumptions about the potential have to be made.

Starting from the non-linear Schrödinger equation

$$i\hbar \frac{\partial}{\partial t} \Psi(\vec{r}, t) = \left( -\frac{\hbar^2}{2m} \Delta + V(\vec{r}) + \vec{F} \cdot \vec{r} f(t) \right) \Psi(\vec{r}, t) + Ng |\Psi(\vec{r}, t)|^2 \Psi(\vec{r}, t) \quad (\text{A1})$$

with

$$g = \frac{4\pi a \hbar^2}{m}, \quad (\text{A2})$$

we make the ansatz

$$\Psi(\vec{r}, t) = e^{-iE_0 t/\hbar} [c_1(t)u_1(\vec{r}) + c_2(t)u_2(\vec{r})] + e^{-iE_1 t/\hbar} [d_1(t)w_1(\vec{r}) + d_2(t)w_2(\vec{r})]; \quad (\text{A3})$$

without a time-dependent potential difference ( $f(t) = 0$ ) and without interaction ( $g = 0$ ),  $u_{1,2}$  are the single particle wave-functions for particles localized in the ground state of well one/two;  $w_1$  and  $w_2$  are the wave-functions of the first excited states. For the weak coupling in our physical situation, the solutions of the single-particle Schrödinger equation without forcing are given by

$$u_{\pm}(\vec{r}) \simeq \frac{1}{\sqrt{2}} [u_1(\vec{r}) \pm u_2(\vec{r})] \\ w_{\pm}(\vec{r}) \simeq \frac{1}{\sqrt{2}} [w_1(\vec{r}) \pm w_2(\vec{r})]$$

with eigenenergies  $E_0^{\pm}$  for  $u_{\pm}$  and  $E_1^{\pm}$  for  $w_{\pm}$ , and corresponding tunneling splittings:

$$\hbar\Omega = E_0^+ - E_0^- \\ \hbar\Omega_1 = E_1^+ - E_1^-.$$

After inserting Eq. (A3) into Eq. (A1) and projecting the result onto the modes, tedious but straightforward calculations for wells which are given as harmonic oscillators result in the non-linear Schrödinger equation in the four-mode approximation:

$$i\dot{c}_1 = -\frac{\Omega}{2}c_2 + \mu_{10} e^{-i\omega t} f(t)d_1 + [2N\kappa|c_1|^2 + 4N\kappa_{10}|d_1|^2 + \mu f(t)]c_1 \\ i\dot{c}_2 = -\frac{\Omega}{2}c_1 - \mu_{10} e^{-i\omega t} f(t)d_2 + [2N\kappa|c_2|^2 + 4N\kappa_{10}|d_2|^2 - \mu f(t)]c_2 \\ i\dot{d}_1 = -\frac{\Omega_1}{2}d_2 + \mu_{10} e^{-i\omega t} f(t)c_1 + [2N\kappa_1|d_1|^2 + 4N\kappa_{10}|c_1|^2 + \mu f(t)]d_1 \\ i\dot{d}_2 = -\frac{\Omega_1}{2}d_1 - \mu_{10} e^{-i\omega t} f(t)c_2 + [2N\kappa_1|d_2|^2 + 4N\kappa_{10}|c_2|^2 - \mu f(t)]d_2. \quad (\text{A4})$$

For the interaction parameters  $\hbar\kappa = \frac{g}{2} \int |u_{1,2}|^4 d^3r$ ,  $\hbar\kappa_1 = \frac{g}{2} \int |w_{1,2}|^4 d^3r$  and  $\hbar\kappa_{10} = \frac{g}{2} \int |u_{1,2}|^2 |w_{1,2}|^2 d^3r$  we obtain:

$$\hbar\kappa_1 = \frac{3}{4}\hbar\kappa \\ \hbar\kappa_{10} = \frac{1}{2}\hbar\kappa.$$

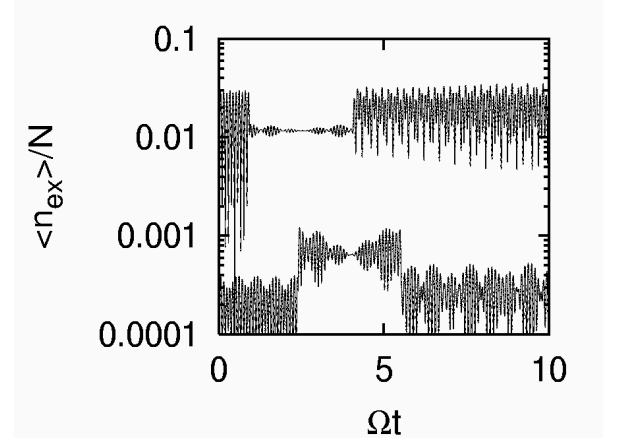


FIG. 4: Tunneling beyond the two-mode approximation: fraction of particles which can be found in the first two excited energy levels. The data was obtained by numerically solving the non-linear Schrödinger equation in four-mode approximation for the same situation as considered before in Fig 2. Top:  $\mu_1 = -1.8\Omega$  and  $\mu_0 = 10\mu_1$ . Bottom:  $\mu_1 = -2.05\Omega$  and  $\mu_0 = \mu_1$ . In both cases the parameters discussed in Sec. II are used.

Furthermore, we have:

$$\mu_{10} = \mu \frac{\ell_{\text{osc}}}{d}$$

(where  $\frac{\ell_{\text{osc}}}{d}$  is the ratio of the oscillator length and half the distance of the two potential minima). The tunneling splittings are given by (*cf.* [23, 24]):

$$\hbar\Omega \simeq \hbar\omega \sqrt{2/\pi} d/\ell_{\text{osc}} \exp(-0.5d^2/\ell_{\text{osc}}^2), \\ \hbar\Omega_1 = \hbar\Omega \left( \frac{d^2}{\ell_{\text{osc}}^2} - 2 \right).$$

In the derivation of Eq. (A4) we used:

$$\int u_1(\vec{r}) \vec{r} u_1(\vec{r}) = \vec{d} \\ \int u_2(\vec{r}) \vec{r} u_2(\vec{r}) = -\vec{d} \\ \int w_1(\vec{r}) \vec{r} w_1(\vec{r}) = \vec{d} \\ \int w_2(\vec{r}) \vec{r} w_2(\vec{r}) = -\vec{d}$$

where  $2\vec{d}$  is the vector connecting the two potential minima.

Within the two-mode approximation, coupling to the higher energy levels is neglected and the equations simplify to:

$$i\dot{c}_1 = -\frac{\Omega}{2}c_2 + 2N\kappa|c_1|^2c_1 + \mu f(t)c_1 \quad (\text{A5}) \\ i\dot{c}_2 = -\frac{\Omega}{2}c_1 + 2N\kappa|c_2|^2c_2 - \mu f(t)c_2$$

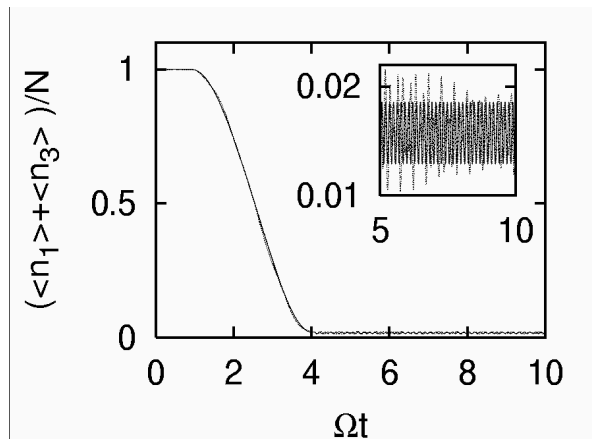


FIG. 5: Transfer of the condensate between the wells: two-mode approximation (solid line) versus four-mode approximation (dotted line) for  $\mu_1 = -1.8\Omega$  and  $\mu_0 = 10\mu_1$  (with the same time-dependent potential variation as in Fig. 2) and the parameters discussed in Sec. II. Although the fraction of particles transferred to the excited states is of the order of one percent (see top curve in Fig. 4), the quality of the transfer between the wells differs only very slightly between both models (see inset).

In Fig. 4 the fraction of particles excited to the two upper energy levels is plotted as a function of time, for the same situation as considered before in Fig. 2. While for the case with an initial offset of  $\mu_1 = -2.05\Omega$  and  $\mu_0 = \mu_1$  (cf. Eq. (12)), the degree of excitation lies below 0.1%, it is a order of magnitude larger for  $\mu_1 = -1.8\Omega$  and  $\mu_0 = 10\mu_1$ . Still, even in this case the transfer between the wells differs only very slightly between both models (see Fig. 5).

- 
- [1] M. R. Andrews, C. G. Townsend, H. J. Miesner, D. S. Durfee, D. M. Kurn, and W. Ketterle, *Science* **275**, 637 (1997).
- [2] Y. Castin and J. Dalibard, *Phys. Rev. A* **55**, 4330 (1997).
- [3] A. Smerzi, S. Fantoni, S. Giovanazzi, and S. R. Shenoy, *Phys. Rev. Lett.* **79**, 4950 (1997).
- [4] S. Raghavan, A. Smerzi, S. Fantoni, and S. R. Shenoy, *Phys. Rev. A* **59**, 620 (1999).
- [5] F. S. Cataliotti, S. Burger, C. Fort, P. Maddaloni, F. Minardi, A. Trombettoni, A. Smerzi, and M. Inguscio, *Science* **293**, 5531 (2001).
- [6] F. Meier and W. Zwerger, *Phys. Rev. A* **64**, 033610 (2001).
- [7] L. Salasnich, A. Parola, and L. Reatto, *J. Phys. B* **35**, 3205 (2003).
- [8] F. Grossmann, T. Dittrich, P. Jung, and P. Hänggi, *Phys. Rev. Lett.* **67**, 516 (1991).
- [9] N. Tsukada, M. Gotoda, Y. Nomura, and T. Isu, *Phys. Rev. A* **59**, 3862 (1999).
- [10] M. Albiez, R. Gati, J. Foelling, S. Hunsmann, M. Cristiani, and M. K. Oberthaler, *Phys. Rev. Lett.* **95**, 010402 (2005).
- [11] C. Monroe, D. M. Meekhof, B. E. King, and D. J. Wineland, *Science* **272**, 1131 (1996).
- [12] L. Deng, E. W. Hagley, J. Wen, M. Trippenbach, Y. Band, P. S. Julienne, J. E. Simsarian, K. Helmerson, S. L. Rolston, and W. D. Phillips, *Nature* **398**, 218 (1999).
- [13] O. Mandel, M. Greiner, A. Widera, T. Rom, T. W. Hänsch, and I. Bloch, *Nature* **425**, 937 (2003).
- [14] J. I. Cirac, M. Lewenstein, K. Mølmer, and P. Zoller, *Phys. Rev. A* **57**, 1208 (1998).
- [15] K. Mølmer and A. Sørensen, *Phys. Rev. Lett.* **82**, 1835 (1999).
- [16] A. Sørensen, L. M. Duan, J. I. Cirac, and P. Zoller, *Nature* **409**, 63 (2001).
- [17] J. A. Dunningham and K. Burnett, *J. Mod. Opt.* **48**, 1837 (2001).
- [18] A. Micheli, D. Jaksch, J. I. Cirac, and P. Zoller, *Phys. Rev. A* **67**, 013607 (2003).
- [19] K. W. Mahmud, H. Perry, and W. P. Reinhardt, *J. Phys. B* **36**, L265 (2003).
- [20] R. S. Judson and H. Rabitz, *Phys. Rev. Lett.* **68**, 1500 (1992).
- [21] A. Assion, T. Baumert, M. Bergt, T. Brixner, B. Kiefer, V. Seyfried, M. Strehle, and G. Gerber, *Science* **282**, 919 (1998).
- [22] A. S. Parkins and D. F. Walls, *Physics Reports* **303**, 1 (1998).
- [23] G. J. Milburn, J. Corney, E. M. Wright, and D. F. Walls, *Phys. Rev. A* **55**, 4318 (1997).
- [24] M. Holthaus and S. Stenholm, *Europhys. J. B* **20**, 451 (2001).
- [25] J. C. Eilbeck, P. S. Lomdahl, and A. C. Scott, *Physica D* **16**, 318 (1985).
- [26] V. M. Kenkre and D. K. Campbell, *Phys. Rev. B* **34**, R4959 (1986).
- [27] G. Kalosakas, A. R. Bishop, and V. M. Kenkre, *Phys. Rev. A* **68**, 023602 (2003).
- [28] L. F. Shampine and M. K. Gordon, *Computer solution of ordinary differential equations: the initial value problem* (Freeman, San Francisco, 1975).
- [29] V. I. Yukalov, *Phys. Rev. Lett.* **90**, 167905 (2003).
- [30] D. S. Hall, M. R. Matthews, C. E. Wieman, and E. A. Cornell, *Phys. Rev. Lett.* **81**, 1543 (1998).